DOR: 20.1001.1.27170314.2021.10.2.3.4

Research Paper

The Effect of ECAP Die Helix Angle on the Microstructure Homogeneity of the Processed Samples by FEM Method

Amir Neshastegir Kashi[1], Farshid Ahmadi[*1]
[1]Department of Mechanical Engineering, University of Kashan, Kashan, 8731753153, Iran
Email of Corresponding Author: fa.ahmadi@kashanu.ac.ir
Received: June 25, 2021; Accepted: August 13, 2021

Abstract
Equal channel angular pressing is one of the most popular processes for the fabrication of ultrafine-grained (UFG) materials. Homogeneous strain distribution is one of the main expected outputs in this process. Recently, a new modification has been applied on the ECAP die in which the workpiece undergoes twisting in the exit channel which is defined as the helix angle of the die. In this paper, the effect of the helix angle in the exit channel along with other effective parameters, including friction coefficient and die channel angle was investigated by the FEM method. At first, a FEM model was developed based on available experimental data. Having verified the FEM model, Taguchi's design of the experimental approach was employed in which the helix angle and friction coefficient had four levels and the die channel angle had two levels. Evaluating the obtained results by the ANOVA method showed that the p-value of the helix angle was 0.01 i.e., the helix angle was an effective parameter on strain distribution and maximum imposed strain. The results also showed that the homogeneity of strain distribution decreases with increasing the friction coefficient and the helix angle and increases with increasing the die channel angle. Also, increasing the helix angle led to an increase in the maximum imposed strain.

Keywords
ECAP, Helix angle, Frictional Coefficient, Die Angle, Taguchi Approach, Homogeneity

1. Introduction
Equal channel angular pressing (ECAP) is one of the most attractive processes for the fabrication of ultrafine-grained (UFG) material among severe plastic deformation techniques. It was first introduced in Russia by Segal in 1977 [1, 2]. In this process samples with rectangular or round cross-sections are put in the entry channel and pressed to the exit channel as shown in Figure 1. Therefore, severe plastic deformation is induced on the sample which changes the microstructure and mechanical properties of the deformed sample.

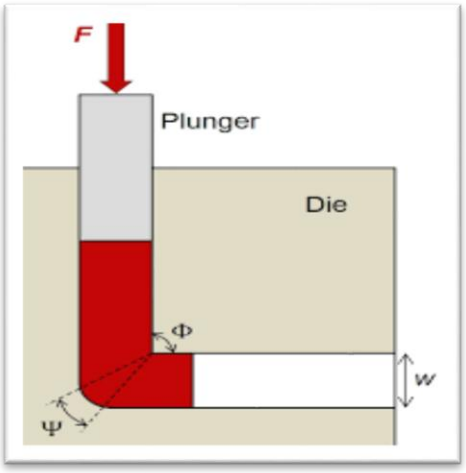

Figure 1. Schematic drawing of ECAP

Nemati et al. [3] studied the properties of deformed samples for pure copper at various strain rates. Results indicated that the ultimate strength increased after eight passes around 100%. The amount of increase in hardness after eight passes was 36%. Also, the elongation increased after the sixth and eighth passes while decreased for the second and fourth passes. Ahmadi and Farzin investigated the effect of superimposing ultrasonic vibration on the punch during the equal channel angular pressing process by finite element method [4]. The results proved that the forming force was reduced by ultrasonic vibration. The amount of reduction force depends on the vibration amplitude. Many FEM-based analyses have been done to determine strain distribution and deformation behavior. Chung et al. investigated the homogeneity of microstructure obtained in the ECAP process [5]. They indicated that the effective strain of the billet after the ECAP process was not homogeneous. Investigations of Kim and Namkung [6] illustrated that routes BA gives the lowest strain distribution homogeneity while employing routes of C and BC leads to the highest strain homogeneity. Mahallawy et al. [7] investigated the influences of different numbers of ECAP passes on strain homogeneity of Al with Cu contents 0-5% by finite element method. The results showed that the strain homogeneity increased with increasing the ECAP passes number. Djavanroodi et al. examined the deformation behavior of commercially pure aluminum in ECAP by finite element method [8]. They studied the effect of various die channel angles, low-friction, and high-friction conditions, and back punch pressure on strain uniformity and strain level. The results indicated that strain uniformity and strain level increased with decreasing the channel angle or increasing the friction coefficient between the sample surface and die surface or imposing back punch pressure in the exit channel. Lu et al. [9] have evaluated the strain homogeneity of aluminum alloys HS6061-T6 by using finite element method for a various channel angles with the consideration of friction coefficient and strain hardening of material. They showed that the maximum strain uniformity was obtained for $\varphi = 110^{\circ}$ in comparison with other channel angles. Djavanroodi et al. [10] proposed a new method to increase the strain uniformity by inserting cylindrical aluminum samples in the commercial pure copper tube. Comparison of the results showed that using this method improved the microstructure homogeneity compared to the conventional method. Zhang et al. [11] investigated the effect of inner fillet radius on effective strain homogeneity in equal channel angular pressing. The results showed that the inner fillet radius had significant effect on both the quantity and distribution of effective strain. By increasing the inner fillet radius, the effective strain in both the inner and outer region is reduced. Ahmadi et al. [12]

proposed a new route for the ECAP process consisting of a combination of routes B_c and C. Their results indicated that the strain homogeneity obtained by the proposed route was better than other conventional routes Nejadseyfi et al. [13] introduced the new lambda(λ)angle in the equal channel angular pressing. Lambda angle was characterized as a clockwise angle between the theoretical shear plane and the punch billet interface. Their results show $\lambda = 90^\circ$ leads to higher homogeneity compared to the conventional method with $\lambda = 45^\circ$. This is due to the reduced width of the plastic deformation zone (PDZ). By reducing the width of PDZ, the induced shear strain becomes homogenous resulting in more uniform microstructure. Different types of lambda angle are shown in Figure 2.

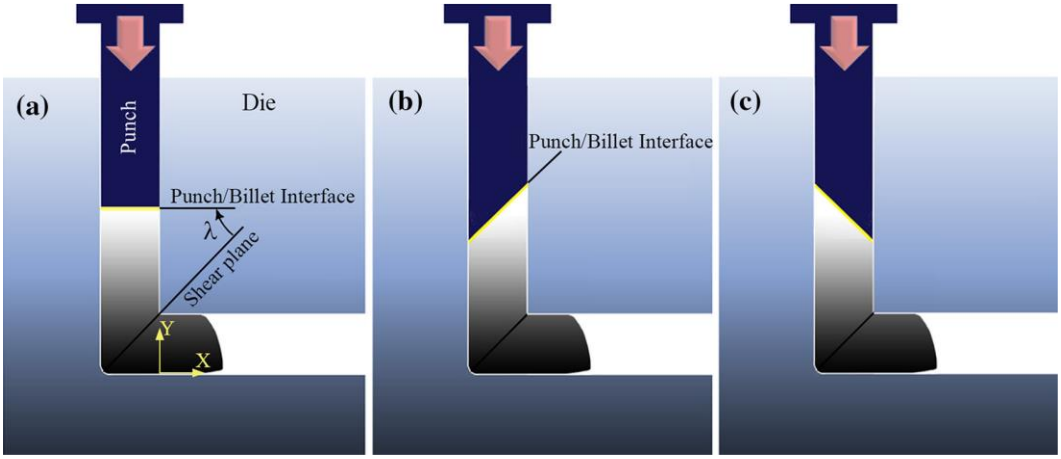

Figure 2. (a) $\boldsymbol{\lambda = 45^\circ}$, (b) $\boldsymbol{\lambda = 0^\circ}$, (c) $\boldsymbol{\lambda = 90^\circ}$ [7]

Ahmadi et al. [14] showed imposing ultrasonic vibrations on conventional ECAP could significantly enhance the grain refinement. They investigated processed samples with and without ultrasonic vibrations. After applying the ECAP process on the samples without using ultrasonic vibrations the grains were refined to 45 µm, while in the presence of ultrasonic vibrations with the amplitudes of 2.5 and 5 µm, the grains were further refined to 28.2 and 22 µm, respectively. By increasing vibration amplitudes, the homogeneity of the microstructure increased. Shaban [15] evaluated the effects of strain hardening exponent (n) and strain rate sensitivity (m) on the plastic strain distribution by finite element simulation. The results revealed that the effect of m and n values on plastic strain was more pronounced at downside areas of the sample in comparison with upper areas. Also, by decreasing strain hardening exponent at a constant strain rate sensitivity, plastic strain increases. Recently, some modifications of the ECAP process such as the non-equal channel lateral extrusion (NECLE) [16], incremental ECAP [17], and the twist channel angular pressing [18] have been studied aiming to increase the efficiency of the ECAP process. In this regard, Snopinski el al. proposed a new ECAP die with a helix angle of 30° in the exit channel [19]. They indicated that this modification in ECAP dies improved grain refinement due to the vortex-like flow of metal during subsequent deformations. The mechanical properties of the processed samples enhanced significantly after the first pass of ECAP, while there was no significant increase in the subsequent passes.

Since Snopinsky in his experimental work only dealt with the effect of one helix angle i.e., helix angle of 30°, the objective of this paper is to investigate the effect of different helix angles on the homogeneity of the microstructure and the value of imposed strain along with changing other parameters including

friction conditions and die channel angle. This investigation is based on FEM analyses and analysis of variance (ANOVA). However, numerical results are validated by available experimental data.

2. FEM analysis

The material used for this research was commercial Al-3%Mg alloy. The initial dimensions of the billet were 14.75 mm × 14.75 mm × 50 mm. The material and geometrical dimensions of the billet considered in the FEM model were in accordance with Snopinski's experimental work. An initial model that included 33000 elements using the C3D8R and ALE re-meshing technique was employed during all simulations. For simplicity, the dies were considered to be rigid. The studied parameters were friction coefficient, channel angle, and helix angle. ECAP die with the helix angle of 30° in the exit channel as well as the corresponding FEM model are shown in Figure 3.

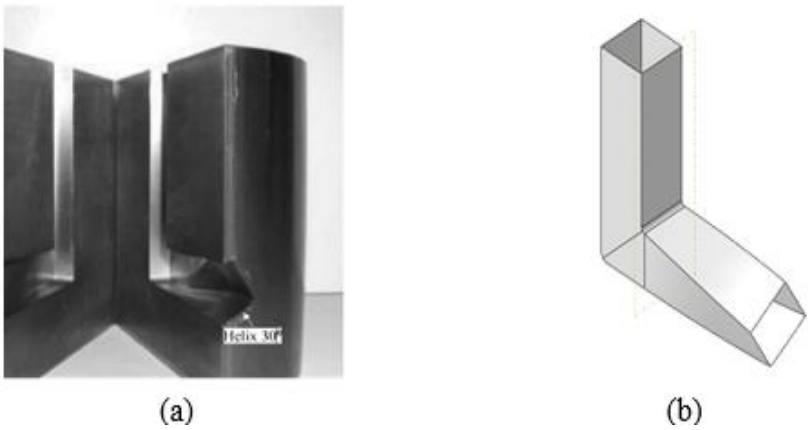

Figure 3. Modified ECAP die with helix angle of 30º in the exit channel (a) experimental study [19], (b) FEM study

The ECAPed samples for both numerical simulation and experimental procedure for helix angle of 30º are shown in Figure 4.

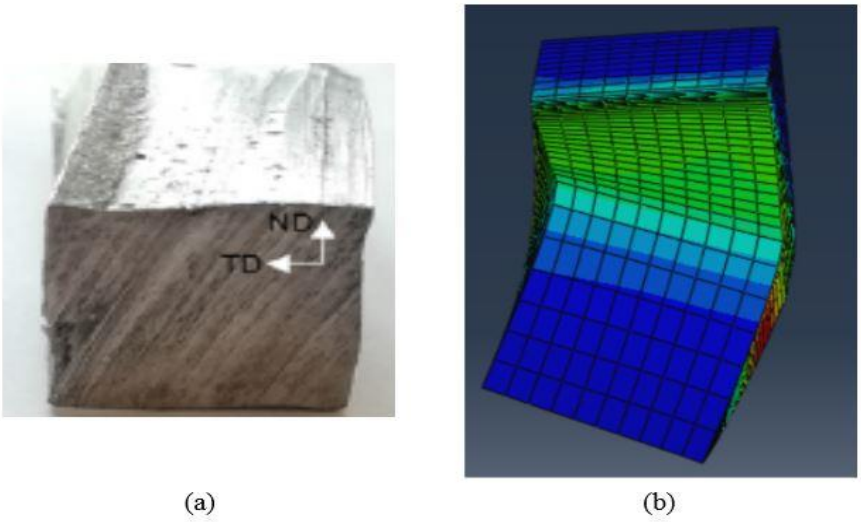

Figure 4. ECAPed sample obtained by (a) Experimental study (b) FEM model

To validate the FEM model, the standard deviation of the effective strains at the points in the middle section of the model corresponding to the measurement points for microhardness in the experimental work was considered. For this purpose, a path in the middle section of the FEM model was created and the standard deviation of effective strains was calculated in this path. As already mentioned, the path corresponds to the measurement path for microhardness in the experimental work. The mentioned path is shown in Figure 5.

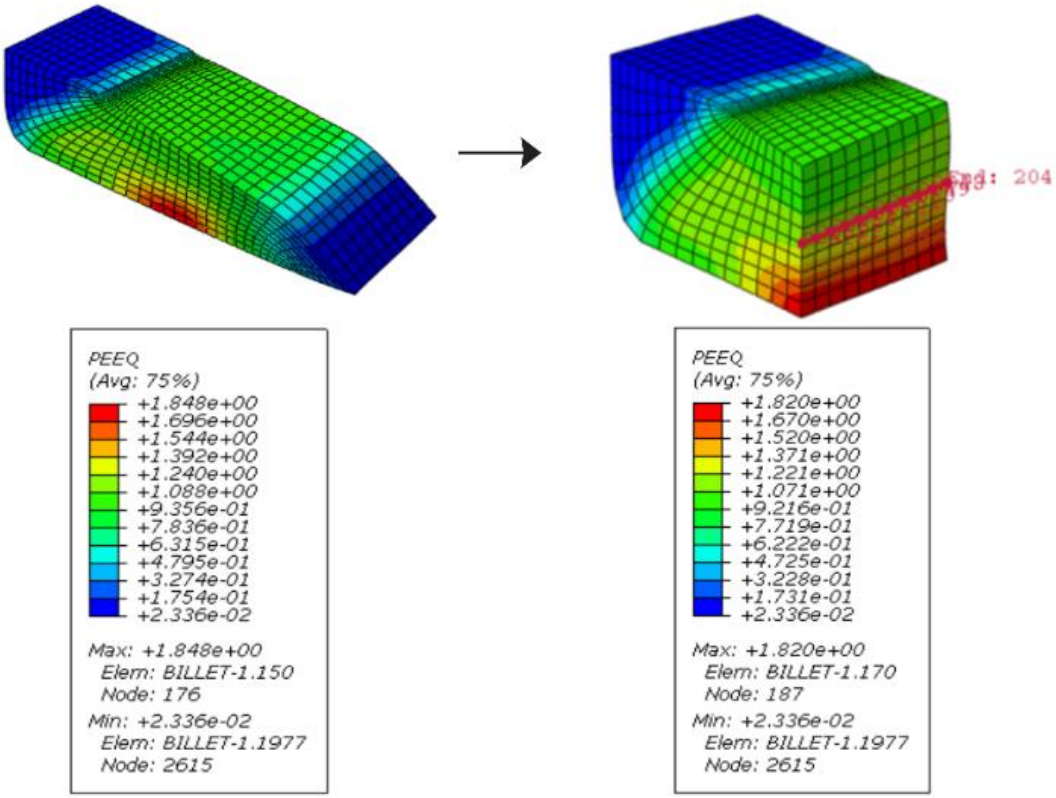

Figure 5. The path generated in the middle cross-section to calculate the standard deviation of strains according to the path created in the experimental study for measurement of hardness

Figure 6 also shows the graph of the effective strain values on the path, as well as the micro-hardness values measured by Snopinski [19] on a path corresponding to the path defined in the FEM model. Since the strain values are in the range of 1 to 1.5 and microhardness values are in the range of 90 to 100 Vickers, it is not reasonable to compare the standard deviation of them with each other. Hence, to compare the microstructure homogeneity of the ECAPed sample and FEM model, the ratio of the standard deviation to the mean was considered for both strain and microhardness values. These ratios for microhardness values in experimental work and also for effective plastic strains in the FEM model are presented in Table 1.

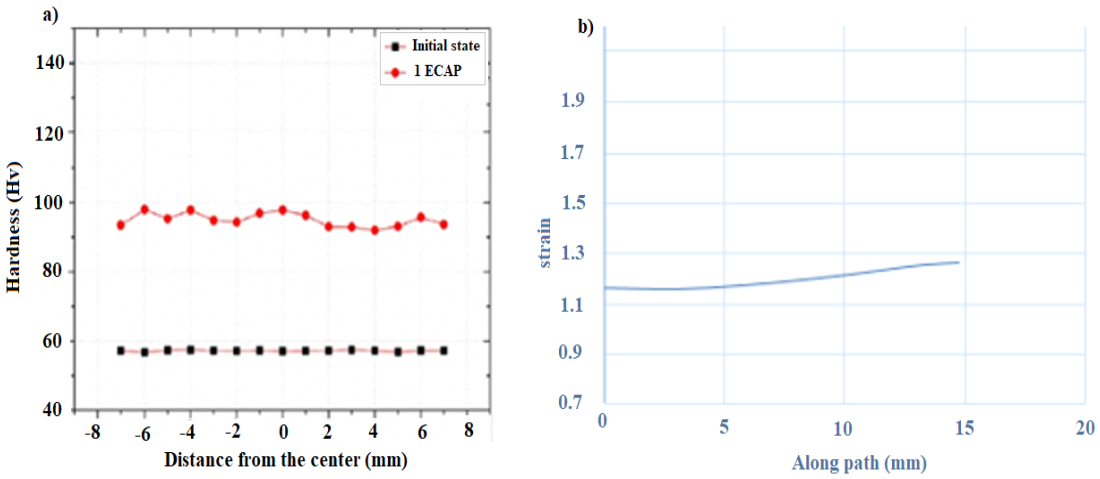

Figure 6. (a) Different measured hardness in the sample for the initial sample and after one pass [19], (b) strain calculated at nodes in FEM

Table 1. Numerical and experimental results

	Numerical results (for effective strain values)	Experimental results (for micro-hardness values)
The ratio of Standard deviation to the mean	3.9405	3.203521

Now that the FEM results and experimental data are in very good agreement, investigation of the effect of the other parameters such as channel angles, helix angles, and friction coefficients are considered in FEM simulations and based on a design of experiments. In this research for helix angle and friction coefficient four levels and for channel angle two levels are considered. The set of parameters used in this paper are shown in Table 2. FEM model of ECAP dies with Various helix angles are shown in Figure 7.

Table 2. Investigated parameters

Level	Helix angle (∘)	Friction coefficient	Channel angle (∘)
1	0	0	90
2	15	0.025	120
3	30	0.05	-
4	45	0.1	-

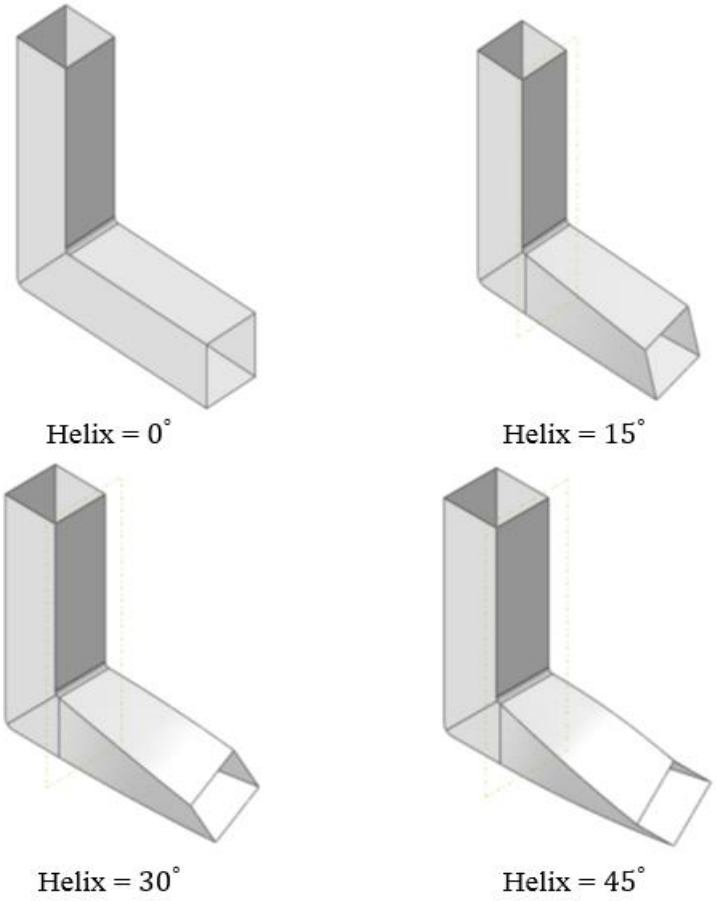

Figure 7. FEM model of ECAP dies with various helix angles

In general, there are two approaches to express the strain distribution. The first is the inhomogeneity index c_i defined by Li et al. [20]:

$$c_i = \frac{\varepsilon_{max} - \varepsilon_{min}}{\varepsilon_{avg}} \quad (1)$$

Where ε_{max},ε_{min} and ε_{avg} are the maximum, minimum, and average equivalent plastic strain, respectively. Fewer magnitudes of c_i means better homogeneity. According to Eq. (1), only the difference between two extreme values of the strain is used. The second method called standard deviation (S.D.) [11]. In this study, S.D. has been utilized to measure strain homogeneity.

$$S.D = \sqrt{\frac{\sum_{i=1}^{n} \left(\overline{\varepsilon}_i - \overline{\varepsilon}_{avg}\right)^2}{n}} \quad (2)$$

Where $\overline{\varepsilon}_i$, $\overline{\varepsilon}_{avg}$ are the plastic strain magnitude at each node and the average value of plastic strains of all the nodes respectively, and n is the number of all the nodes. Higher values of S.D. indicate more non-uniformity. In this paper, the standard deviation values were calculated for all elements in the middle cross-section of the sample.

3. FEM results

According to the design of the experiment based on Taguchi's method, 16 FEM models were prepared and implemented to investigate the effect of helix angle, friction coefficient and channel angle on maximum imposed strain and strain homogeneity after the ECAP process. The details of the simulations and their results are shown in Table 3. The standard deviations of the equivalent plastic strain values in the middle cross-section of the billet were also reported in Table 3. For example, the contours of the equivalent plastic strain of ECAPed billet and middle cross-section of the billet under the condition of $\mu = 0.05$, helix angle = 30° and $\phi = 90°$ are shown in Figure 8.

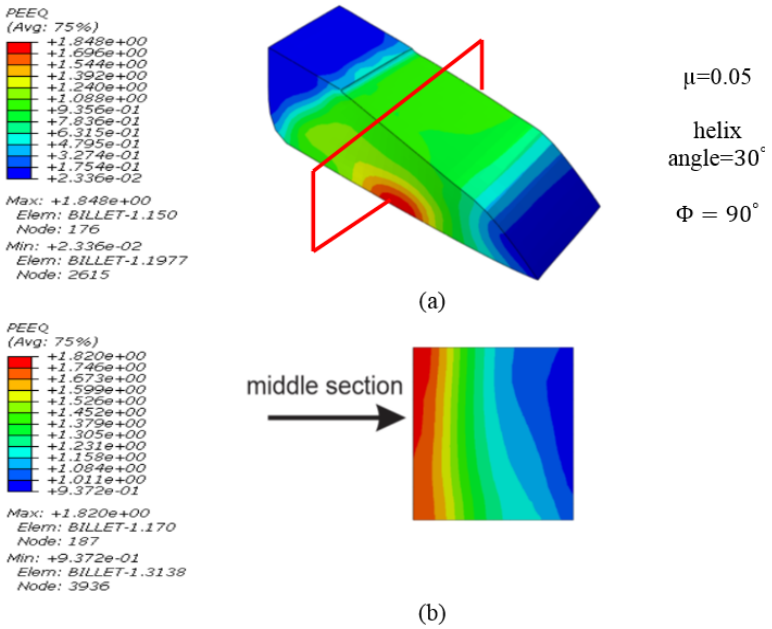

Figure 8. (a) Equivalent plastic strain contours of deformed part, (b) equivalent plastic strain contours in the middle cross-section

Table 3. Obtained results from simulations

Test	μ	ϕ	Helix angle	Standard deviation	Maximum strain
1	0	90	0	0.042487	1.377
2	0	90	15	0.034890	1.392
3	0	120	30	0.082017	0.9216
4	0	120	45	0.075623	0.9437
5	0.025	90	0	0.060200	1.466
6	0.025	90	15	0.109900	1.55
7	0.025	120	30	0.080500	0.8746
8	0.025	120	45	0.071640	0.89
9	0.05	120	0	0.100743	0.897
10	0.05	120	15	0.090145	0.9021
11	0.05	90	30	0.253695	1.848
12	0.05	90	45	0.294800	1.941
13	0.1	120	0	0.105000	1.02
14	0.1	120	15	0.086297	1.003
15	0.1	90	30	0.462930	2.513
16	0.1	90	45	0.487900	2.17

For investigating the effects of influencing parameters including helix angle, friction coefficient, and channel angle on standard deviation and maximum imposed strain, an analysis of variance (ANOVA) method was employed.

Table 4 shows the analysis of variance for standard deviation values as the response of the tests. As it can be seen the p-values for all three parameters are less than 0.05. Therefore, it proves that all three parameters are effective in the strain distribution. According to the F-values, the most effective parameters on strain homogeneity is the die channel angle and then friction coefficient and helix angle, respectively.

Table 4. Analysis of variance for standard deviation values

Source	DF	Seq SS	Adj MS	Adj MS	F value	P-value
μ	3	0.130829	0.043620	0.130829	14.68	0.001
helix	3	0.087286	0.029095	0.087286	9.79	0.005
ϕ	1	0.069543	0.069543	0.069543	23.41	0.001
Error	8	0.023767	0.002791	0.023767		
Total	15	0.311425				
R-Sq = 92.67%			R-Sq(adj) = 85.69%			

The main effect plots for standard deviation are shown in Figure 9. The results show that by increasing helix angle and friction coefficient the standard deviation also increases while increasing channel angle results in decreasing the standard deviation of equivalent plastic strain in the middle cross-section meaning more homogeneity.

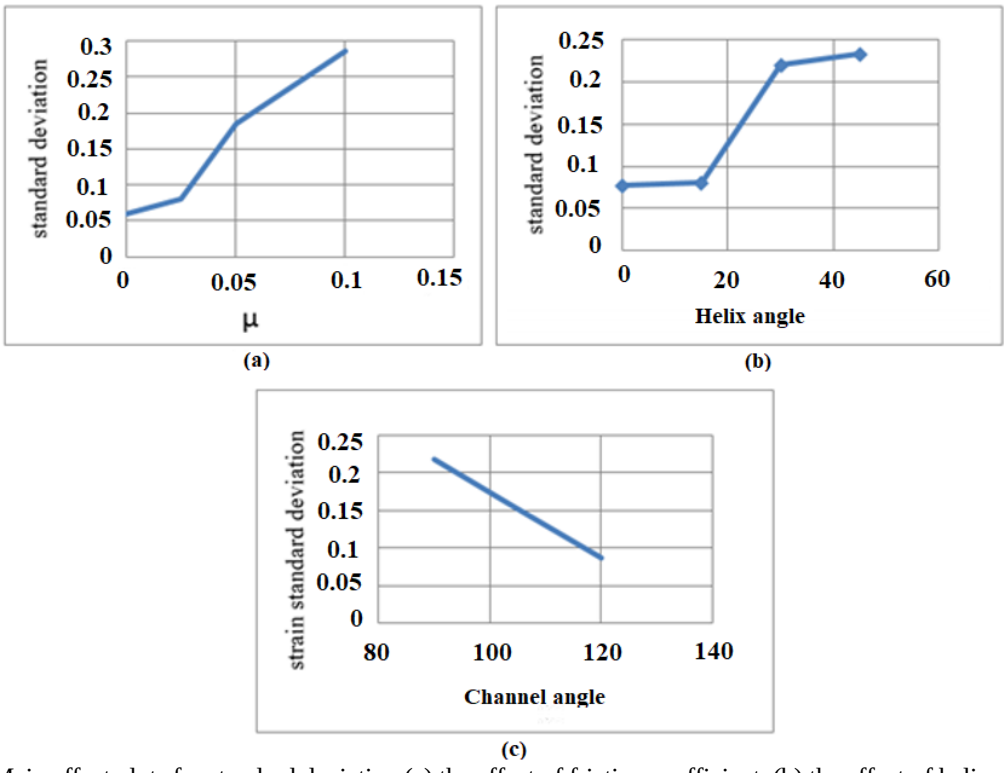

Figure 9. Main effect plots for standard deviation (a) the effect of friction coefficient, (b) the effect of helix angle, (c) the effect of channel angle

A linear regression model was utilized to express the relation between the standard deviation as the homogeneity index and effective parameters.

$$S.D = 0.417968 + 2.4090x_1 + 0.00403751x_2 + 0.00439515x_3 \quad (3)$$

Wherex_1, x_2 and x_3 are friction coefficient, helix angle in the exit channel, and die channel angle, respectively. Analysis of variance for maximum strain values is also shown in Table 5Table **1**. The most effective parameters on maximum imposed strain are the channel angle than the helix angle and the friction coefficient, respectively. It is shown that the effect of helix angle on maximum imposed strain is greater than that of the friction, while the effect of friction on homogeneity was greater than helix angle.

Table 5. Analysis of variance for maximum strain

Source	DF	Seq SS	Adj MS	Adj MS	F value	P-value
μ	3	1.06854	0.35618	1.06854	13.73	0.002
helix	3	0.058593	0.19513	0.058593	7.52	0.010
ϕ	1	3.36264	3.36264	3.36264	129.6	0.000
Error	8	0.20756	0.02595	0.20756		
Total	15	5.22413				
R-Sq = 96.03%			R-Sq(adj) = 92.55%			

The main effect plots for maximum strain are shown in Figure 10. As can be observed the maximum strain increases by increasing helix angle and friction coefficient while it decreases by increasing channel angle.

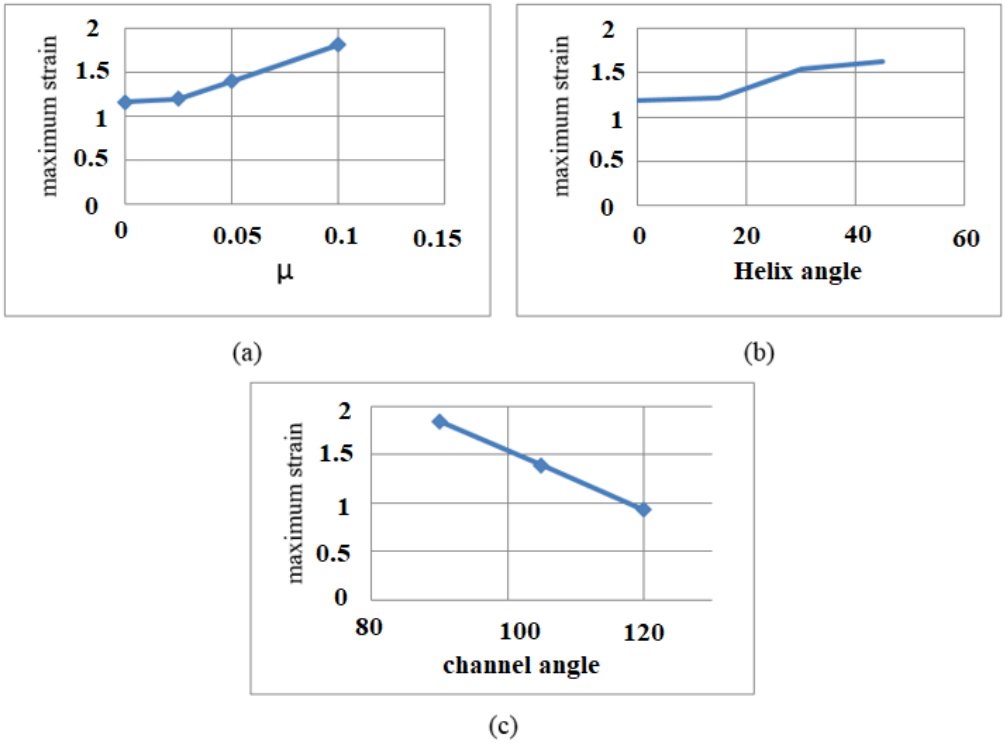

Figure 10. The main effect plots for the mean of maximum strain (a) the effect of friction coefficient, (b) the effect of helix angle, (c) the effect of channel angle

In this paper, to determine the effect of helix angle on punch force, a series of simulations were also carried out. For this purpose, simulations were implemented for four-helix angles of 0°,15°, 30°and 45°. The friction coefficient and channel angle were 0.05 and 90°, respectively. The force diagrams for four different helix angles are shown in Figure 11. As it can be seen, all four diagrams have the same trend. The maximum force for each helix angle is presented in Table 6. There is a little difference between maximum forces. It can be concluded that the helix angle has a minor effect on force punch during the equal channel angular pressing.

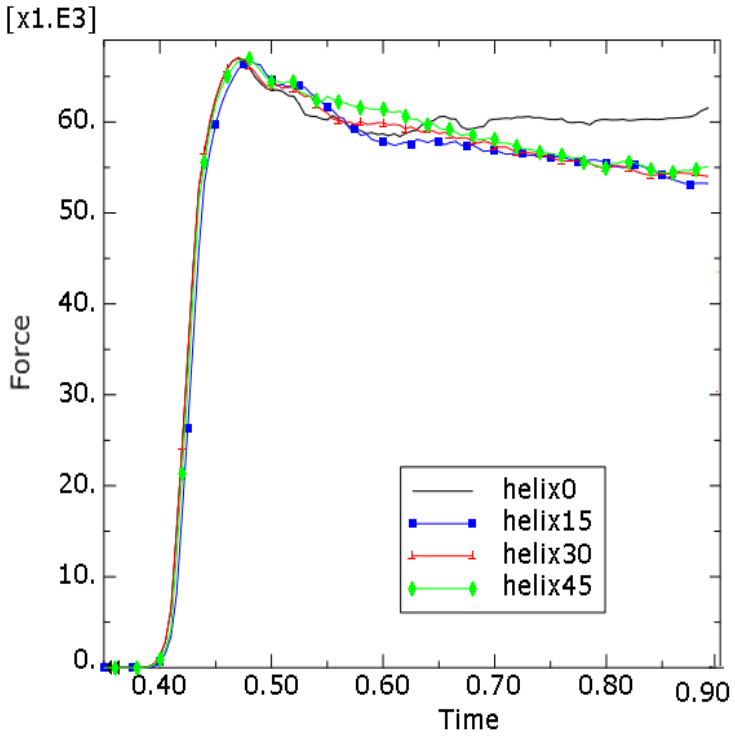

Figure 11. Force diagrams for four different helix angles

Table 6. Maximum force calculated for different helix angles

Helix angle (∘)	0	15	30	45
Maximum force(N)	67794	67394	67606	68054

4. Conclusion

In this research, the influence of helix angle in ECAP die along with other effective parameters i.e., friction coefficient and die channel angle, on strain homogeneity and the maximum imposed strain was studied by using finite elements. The main results of this study are as follows:

1) Evaluating the strain values in the middle cross-section of the billets indicated that the standard deviation of strains calculated for helix angles of 0^o, 15^o, 30^o, and 45^o were 0.077, 0.0803, 0.2197, and 0.2324, respectively. It is concluded that by increasing the helix angle, the strain homogeneity decreases. Also, strain homogeneity decreases by increasing the friction coefficient while increases by increasing the channel angle.

2) Maximum imposed strain is another parameter that was considered in the simulations. It was observed that increasing the helix angle (when the other parameters are constant) results in an increase in the

maximum imposed strain such that the maximum strain for helix angles of 0^o to 45^o increases from 1.19 to 1.62. Also, the maximum imposed strain increases by increasing the friction coefficient and decreasing the channel angle.

3) The results also showed that the helix angle had a minor effect on the force process during the ECAP process.

5. References

[1] Segal, V. 1995. Materials processing by simple shear. Materials Science and Engineering: A. 197(2): 157-164.

[2] Segal, V. 1999. Equal channel angular extrusion: From macromechanics to structure formation. Materials Science and Engineering: A. 271(1-2): 322-333.

[3] Nemati, J., Majzoobi, G., Sulaiman, S., Baharudin, B. and Hanim, M.A. 2014. Finite element and metallurgical study of properties of deformed pure copper by ecae at various strain rates. Proceedings of the Institution of Mechanical Engineers, Part C: Journal of Mechanical Engineering Science. 228(9): 1461-1473.

[4] Ahmadi, F. and Farzin, M. 2014. Finite element analysis of ultrasonic-assisted equal channel angular pressing. Proceedings of the Institution of Mechanical Engineers, Part C: Journal of Mechanical Engineering Science. 228(11): 1859-1868.

[5] Chung, S., Somekawa, H., Kinoshita, T., Kim, W. and Higashi, K. 2004. The non-uniform behavior during ecae process by 3-d fvm simulation. Scripta Materialia. 50(7): 1079-1083.

[6] Kim, W. and Namkung, J. 2005. Computational analysis of effect of route on strain uniformity in equal channel angular extrusion. Materials Science and Engineering: A. 412(1-2): 287-297.

[7] El Mahallawy, N., Shehata, F.A., El Hameed, M.A., El Aal, M.I.A. and Kim, H.S. 2010. 3d fem simulations for the homogeneity of plastic deformation in al–cu alloys during ecap. Materials Science and Engineering: A. 527(6): 1404-1410.

[8] Mogucheva, A., Babich, E., Ovsyannikov, B. and Kaibyshev, R. 2013. Microstructural evolution in a 5024 aluminum alloy processed by ecap with and without back pressure. Materials Science and Engineering: A. 560: 178-192.

[9] Lu, S., Liu, H., Yu, L., Jiang, Y. and Su, J. 2011. 3d fem simulations for the homogeneity of plastic deformation in aluminum alloy hs6061-t6 during ecap. Procedia Engineering. 12: 35-40.

[10] Djavanroodi, F., Daneshtalab, M. and Ebrahimi, M. 2012. A novel technique to increase strain distribution homogeneity for ecaped materials. Materials Science and Engineering: A. 535: 115-121.

[11] Zhang, X. and Cheng, Y. 2017. Influence of inner fillet radius on effective strain homogeneity in equal channel angular pressing. The International Journal of Advanced Manufacturing Technology. 92(9-12): 4001-4008.

[12] Ahmadi, F. and Farzin, M. 2014. Investigation of a new route for equal channel angular pressing process using three-dimensional finite element method. Proceedings of the Institution of Mechanical Engineers, Part B: Journal of Engineering Manufacture. 228(7): 765-774.

[13] Nejadseyfi, O., Shokuhfar, A., Azimi, A. and Shamsborhan, M. 2015. Improving homogeneity of ultrafine-grained/nanostructured materials produced by ecap using a bevel-edge punch. Journal of materials science. 50(3): 1513-1522.

[14] Ahmadi, F., Farzin, M., Meratian, M., Loeian, S. and Forouzan, M. 2015. Improvement of ecap process by imposing ultrasonic vibrations. The International Journal of Advanced Manufacturing Technology. 79(1-4): 503-512.

[15] Ghazani, M.S., Binesh, B. and Fardi-Ilkhchy, A. 2019. Effect of strain rate sensitivity and strain hardening exponent of materials on plastic strain distribution and damage accumulation during equal channel angular pressing. Iranian Journal of Science and Technology, Transactions of Mechanical Engineering. 43(1): 831-844.

[16] Fereshteh-Saniee, F., Asgari, M., Barati, M. and Pezeshki, S.M. 2014. Effects of die geometry on non-equal channel lateral extrusion (necle) of az80 magnesium alloy. Transactions of Nonferrous Metals Society of China. 24(10): 3274-3284.

[17] Chrominski, W., Olejnik, L., Rosochowski, A. and Lewandowska, M. 2015. Grain refinement in technically pure aluminium plates using incremental ecap processing. Materials Science and Engineering: A. 636: 172-180.

[18] Kocich, R., Kunčická, L., Král, P. and Macháčková, A. 2016. Sub-structure and mechanical properties of twist channel angular pressed aluminium. Materials Characterization. 119: 75-83.

[19] Snopiński, P., Tański, T., Matus, K. and Rusz, S. 2019. Microstructure, grain refinement and hardness of al–3% mg aluminium alloy processed by ecap with helical die. Archives of Civil and Mechanical Engineering. 19(2): 287-296.

[20] Li, S., Bourke, M., Beyerlein, I., Alexander, D. and Clausen, B. 2004. Finite element analysis of the plastic deformation zone and working load in equal channel angular extrusion. Materials Science and Engineering: A. 382(1-2): 217-236.